

Thermal order in holographic CFTs and no-hair theorem violation in black branes

Alex Buchel

Department of Applied Mathematics

Department of Physics and Astronomy

University of Western Ontario

London, Ontario N6A 5B7, Canada

Perimeter Institute for Theoretical Physics

Waterloo, Ontario N2J 2W9, Canada

Abstract

We present a large class of holographic models where the boundary $\mathbb{R}^{2,1}$ dimensional conformal field theory has a thermal phase with a spontaneously broken global symmetry. The dual black branes in a Poincare patch of asymptotically AdS_4 violate the no-hair theorem.

May 15, 2020

In [1] the authors asked an interesting question whether an “order” (a thermal phase with a spontaneously broken global symmetry) is always lost at high temperatures¹? There is a number of holographic models known where the answer is “yes”, *i.e.*, there is a critical temperature T_{crit} , such that for $T > T_{crit}$ there is a phase with a spontaneously broken global discrete, \mathbb{Z}_2 , symmetry [2–4] or a continuous, $U(1)$, symmetry [5]. The holographic models mentioned correspond to boundary quantum field theories with a mass scale: a coupling of a relevant operator in the model [2] or a strong coupling scale of the Klebanov-Strassler gauge theory [6] in [5]. Ultimately, it is this mass scale that determines T_{crit} .

But is it possible to have an exotic phenomenon of the global symmetry breaking in the ultraviolet (as first suggested in [2]) in a conformal theory? There is no scale to determine T_{crit} , and the thermal symmetric and the symmetry broken phases must exist for all temperatures. Necessary, the *distinct* holographic duals to these phases — the black branes with the translationary invariant horizons — would violate the no-hair theorem. The purpose of this note is to present explicit examples of such holographic models. An impatient reader can simply jump to the discussion of the holographic models in **Step3**. Rather, we follow the construction route from massive QFTs.

• **Step1**². Consider the effective four-dimensional gravitational bulk action³, dual to a QFT₃ on $\mathbb{R}^{2,1}$,

$$S_{\text{QFT}_3} = S_{\text{CFT}_3} + S_r + S_i = \frac{1}{2\kappa^2} \int dx^4 \sqrt{-\gamma} [\mathcal{L}_{\text{CFT}_3} + \mathcal{L}_r + \mathcal{L}_i], \quad (1)$$

$$\mathcal{L}_{\text{CFT}_3} = R + 6, \quad \mathcal{L}_r = -\frac{1}{2} (\nabla\phi)^2 + \phi^2, \quad \mathcal{L}_i = -\frac{1}{2} (\nabla\chi)^2 - 2\chi^2 - g\phi^2\chi^2, \quad (2)$$

where we split the action into a conformal part S_{CFT_3} ; its deformation by a relevant operator \mathcal{O}_r ; and a sector S_i involving an irrelevant operator \mathcal{O}_i along with its mixing with \mathcal{O}_r under the renormalization group flow, specified by a constant g . In all our numerical analysis we set $g = -100$. The four dimensional gravitational constant κ is related to a central charge c of the UV fixed point as

$$c = \frac{192}{\kappa^2}. \quad (3)$$

¹As in [1], we consider equilibrium phases of the theories without a chemical potential for the conserved global $U(1)$ symmetries.

²This is a review of [2].

³We set the radius of an asymptotic AdS_4 geometry to unity.

We assume the scaling dimension of \mathcal{O}_r to be $\Delta_r = 2$. The scaling dimension of \mathcal{O}_i is $\Delta_i = 4$. Generically, we turn on the non-normalizable coefficient of ϕ , corresponding, the nonzero coupling Λ of the dual operator \mathcal{O}_r . The effective action (1) has a $\mathbb{Z}_2 \times \mathbb{Z}_2$ discrete symmetry that acts as a parity transformation on the scalar fields ϕ and χ . The discrete symmetry $\phi \leftrightarrow -\phi$ is explicitly broken by a relevant deformation of the CFT₃; while the $\chi \leftrightarrow -\chi$ symmetry is broken spontaneously.

The thermal states of the QFT₃ are dual to the black brane solutions in (1) with translationary invariant horizons:

$$ds_4^2 = \frac{\alpha^2 a(x)^2}{(2x - x^2)^{2/3}} \left(-(1-x)^2 dt^2 + [dx_1^2 + dx_2^2] \right) + g_{xx} dx^2, \quad \phi = \phi(x), \quad \chi = \chi(x), \quad (4)$$

where the radial coordinate $x \in (0, 1)$. The constant α is an arbitrary scale parameter, and the metric warp factor g_{xx} is determined algebraically from a, ϕ, ψ . Solving the equations of motion from (1) and (2) with the background ansatz (4), we find,

$$\begin{aligned} a &= 1 - \frac{1}{40} p_1^2 x^{2/3} - \frac{1}{18} p_1 p_2 x + \mathcal{O}(x^{4/3}), \\ \phi &= p_1 x^{1/3} + p_2 x^{2/3} + \frac{3}{20} p_1^3 x + \mathcal{O}(x^{4/3}), \\ \chi &= \chi_4 \left(x^{4/3} + \left(\frac{1}{7} g - \frac{3}{70} \right) p_1^2 x^2 + \mathcal{O}(x^{7/3}) \right), \end{aligned} \quad (5)$$

near the AdS_4 boundary $x \rightarrow 0_+$, and

$$a = a_0^h + a_1^h y^2 + \mathcal{O}(y^4), \quad \phi = p_0^h + \mathcal{O}(y^2), \quad \chi = c_0^h + \mathcal{O}(y^2), \quad (6)$$

near the black brane horizon $y = 1 - x \rightarrow 0_+$. Apart from the overall scaling factor α , a black brane solution is specified with the three UV coefficients $\{p_1, p_2, \chi_4\}$ and the four IR coefficients $\{a_0^h, a_1^h, p_0^h, c_0^h\}$. The UV parameter p_1 determines the coupling constant of the relevant operator \mathcal{O}_r as

$$\Lambda \equiv p_1 \alpha, \quad (7)$$

while the remaining parameters determine the Hawking temperature T of the black brane, its entropy density s , the energy density \mathcal{E} , and the free energy density \mathcal{F} as follows:

$$\begin{aligned} \left(\frac{8\pi T}{\Lambda} \right)^2 &= \frac{6(a_0^h)^3 (6 - 2(c_0^h)^2 + (p_0^h)^2 - g(p_0^h)^2(c_0^h)^2)}{p_1^2 (3a_1^h + a_0^h)}, \quad \frac{\hat{s}}{\Lambda^2} \equiv \frac{384}{c} \frac{s}{\Lambda^2} = \frac{4\pi(a_0^h)^2}{p_1^2}, \\ \frac{\hat{\mathcal{E}}}{\Lambda^3} &\equiv \frac{384}{c} \frac{\mathcal{E}}{\Lambda^3} = \frac{1}{p_1^3} \left(2 - \frac{1}{6} p_1 p_2 \right), \quad \frac{\hat{\mathcal{F}}}{\Lambda^3} \equiv \frac{384}{c} \frac{\mathcal{F}}{\Lambda^3} = \frac{384}{c} \frac{\mathcal{E} - Ts}{\Lambda^3}. \end{aligned} \quad (8)$$

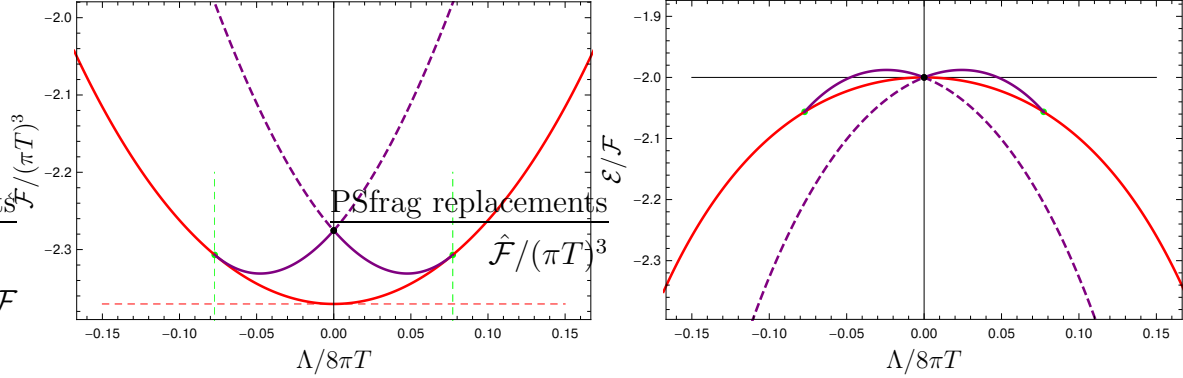


Figure 1: Thermal phases of the QFT_3 with a dual holographic gravitational action (1). The left panel shows the free energy density $\hat{\mathcal{F}}$, see (8), and the right panel shows \mathcal{E}/\mathcal{F} as a function of $\Lambda/(8\pi T)$. At $\Lambda = 0$ the theory has $\mathbb{Z}_2 \times \mathbb{Z}_2$ global symmetry. This symmetry is broken to \mathbb{Z}_2 at $\Lambda \neq 0$ — represented by the red curves. The purple curves represent phases with the spontaneously broken \mathbb{Z}_2 symmetry. They connect with the second order phase transition (green dots, vertical dashed green lines) to a symmetric phase at $T_{\text{crit}} \propto \Lambda$, see (11). The symmetry broken phases (solid purple curves) exist for $T \geq T_{\text{crit}}$ all the way to the infinite temperature. The infinite temperature phase — represented by a black dot — is our first example of the CFT_3 with spontaneously broken global symmetry, see (12). The symmetry breaking phases can be smoothly extended past the infinite temperature — denoted by the purple dashed curves.

Additionally, the thermal expectation values of the operators \mathcal{O}_r and \mathcal{O}_i are given by

$$\langle \mathcal{O}_r \rangle \propto \langle \hat{\mathcal{O}}_r \rangle = p_2, \quad \langle \mathcal{O}_i \rangle \propto \langle \hat{\mathcal{O}}_i \rangle = \chi_4. \quad (9)$$

The latter expectation value, *i.e.*, χ_4 , serves as an order parameter for the spontaneous breaking of the global \mathbb{Z}_2 symmetry.

A selection⁴ of thermal phases of the QFT_3 is presents in fig. 1. Notice that the horizontal axes correspond to $\Lambda/(8\pi T)$, so the region close to the origin corresponds to high temperatures, *i.e.*, $T \gg \Lambda$. We show⁵ the \mathbb{Z}_2 symmetric phases with $\langle \hat{\mathcal{O}}_i \rangle = 0$ (red curves) and the symmetry broken phases $\langle \hat{\mathcal{O}}_i \rangle \neq 0$ (purple curves). The left panel shows the reduced free energy density $\hat{\mathcal{F}}$, see (8). Note that for the AdS_4 -Schwarzschild

⁴There is a tower of the symmetry broken thermal phases similar to those discussed here [2].

⁵In all cases we verified that the first law of thermodynamics $0 = d\mathcal{E}/(Tds) - 1 \Big|_{\Lambda=\text{const}}$ is true numerically to $\sim 10^{-10}$ or better.

black brane

$$\left. \frac{\hat{\mathcal{F}}}{(\pi T)^3} \right|_{red, \Lambda=0} = -\frac{64}{27}, \quad (10)$$

denoted by a red dashed horizontal line. The solid purple curves connect to the red curve with the second-order transition, green dots, at

$$T_{crit} = 0.515597 |\Lambda|, \quad (11)$$

denoted by the green dashed vertical lines. As discovered in [2], the symmetry broken phases exist only in the UV, *i.e.*, for $T \geq T_{crit}$. They extend to infinitely high temperatures, denoted by the black dot. The black dot is our first example of the CFT₃ with the spontaneously broken global discrete symmetry, in this particular case $\mathbb{Z}_2 \times \mathbb{Z}_2$:

$$\text{CFT}_3 : \quad \left. \frac{\hat{\mathcal{F}}}{(\pi T)^3} \right|_{red, \Lambda=0} = -2.275317, \quad \langle \hat{\mathcal{O}}_r \rangle = \pm 0.326946, \quad \langle \hat{\mathcal{O}}_i \rangle = \pm 0.321581, \quad (12)$$

where the uncorrelated \pm signs represent the 4-fold degeneracy of the symmetry broken phases.

In any thermal phase, symmetric or symmetry broken, the equation of state of a CFT₃ is $\mathcal{E} = -2\mathcal{F}$. In the right panel of fig. 1 we plot \mathcal{E}/\mathcal{F} in the QFT₃ as a function of $\Lambda/(8\pi T)$: both the red curve and the purple curves pass through (-2) in the UV (with a numerical accuracy of $\sim 10^{-11}$).

The symmetry broken phases (solid purple curves) can be smoothly extended “past the infinite temperature” — the dashed purple curves. We have been able to reliably construct the dashed purple phases only for $|\Lambda|/(8\pi T) \lesssim 0.2043$.

In fig. 2 we present the order parameter $\langle \hat{\mathcal{O}}_i \rangle$ for the spontaneous breaking of the global \mathbb{Z}_2 symmetry (the left panel), and the thermal expectation value of $\langle \hat{\mathcal{O}}_r \rangle$ (the right panel). The color coding is the same as in fig. 1. Notice that as one lowers the temperature along the dashed purple curves, the absolute value of the order parameter sharply increases as $|\Lambda|/(8\pi T) \rightarrow 0.2043$. This is the main reason why we could not extend these phases to low temperatures⁶.

In fig. 3 we present the speed of the sound waves in various thermal phases of the QFT₃ plasma. The color coding is the same as in fig. 1. All the equilibrium phases, symmetric and with the spontaneously broken \mathbb{Z}_2 symmetry, are thermodynamically and dynamically stable [7]. The speed of the sound waves approach a conformal value in the limit $T/\Lambda \rightarrow \infty$.

⁶We expect that the corresponding black branes have a singular horizon in this limit.

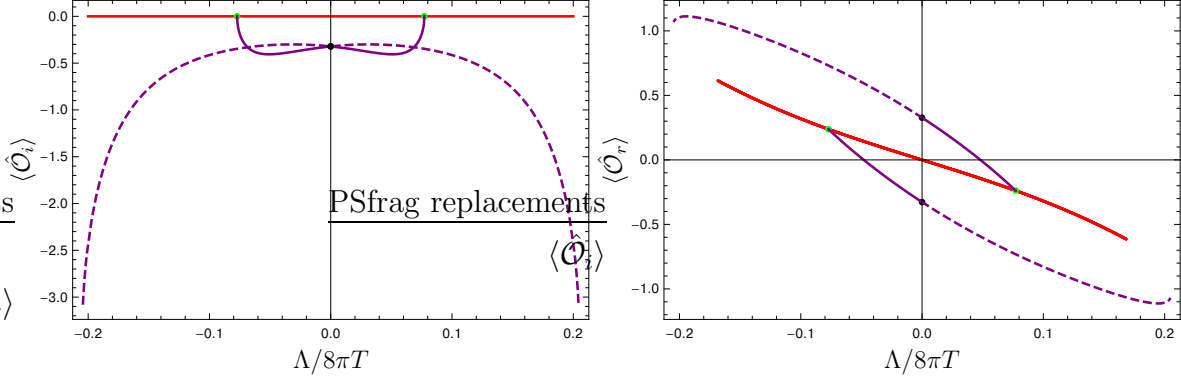


Figure 2: The left panel: the order parameter $\langle \hat{\mathcal{O}}_i \rangle$ for the spontaneous breaking of the global \mathbb{Z}_2 symmetry in the QFT_3 . The right panel: the thermal expectation value of $\langle \hat{\mathcal{O}}_r \rangle$ in the QFT_3 . The color coding is the same as in fig. 1.

An example of a CFT_3 with a spontaneously broken $\mathbb{Z}_2 \times \mathbb{Z}_2$ — the black dot phase in fig. 1 — has a larger free energy density than that of the symmetric phase, dual to the AdS_4 -Schwarzschild black brane:

$$\left. \frac{\hat{\mathcal{F}}}{(\pi T)^3} \right|_{black\ dot} > \left. \frac{\hat{\mathcal{F}}}{(\pi T)^3} \right|_{red, \Lambda=0}. \quad (13)$$

Thus, this phase is metastable⁷. In what follows, we ask the question whether we can introduce an additional “knob” in a holographic model (1) to potential reverse the inequality (13), and have a symmetry broken phase to dominate in a canonical ensemble⁸. This leads up to **Step2**.

- **Step2.** Consider a smooth constant b parameter deformation of the model (1):

$$S_{\text{QFT}_3} \rightarrow S_{\text{QFT}_3^b} \iff \mathcal{L}_i \rightarrow \mathcal{L}_i^b \equiv -\frac{1}{2} (\nabla \chi)^2 - 2\chi^2 - g\phi^2\chi^2 - b\chi^4, \quad (14)$$

with the remaining parts of the effective action left unchanged. Note that the QFT_3^b has the same global symmetries as the QFT_3 . Additionally, the second-order phase transitions associated with the spontaneous breaking of \mathbb{Z}_2 symmetry ($\chi \leftrightarrow -\chi$) happens at T_{crit} given by (11), independent of the deformation parameter b .

⁷It would be extremely interesting to understand the dynamics of the first order phase transition, in particular, to compute the wall tension of the symmetric phase bubble in the symmetry broken thermal phase.

⁸No examples of such models known.

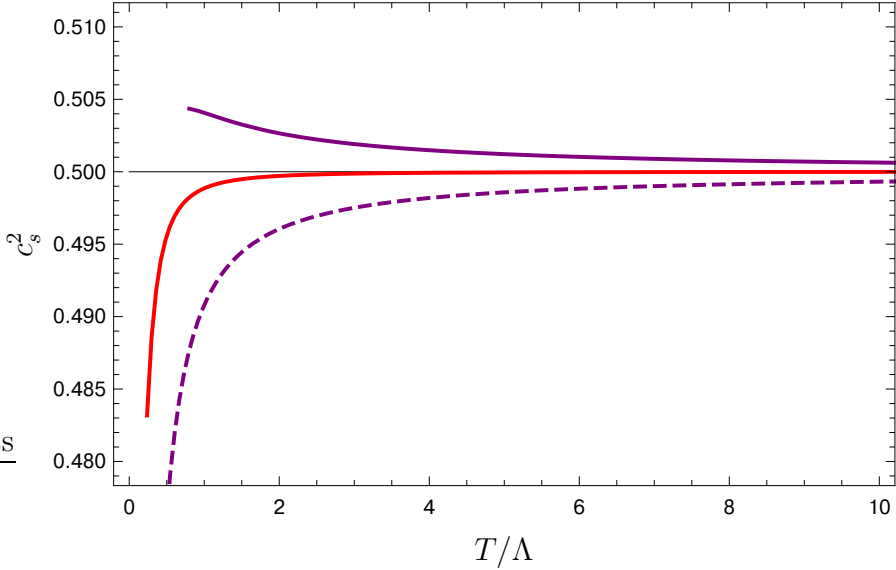


Figure 3: The speed of the sound waves in various equilibrium phases of the QFT_3 plasma. The color coding is the same as in fig. 1.

It is straightforward to repeat the analysis of the thermal phase diagram of the model. In the thermodynamic relations (8) there is only one change⁹:

$$\left(\frac{8\pi T}{\Lambda}\right)^2 = \frac{6(a_0^h)^3(6 - 2(c_0^h)^2 + (p_0^h)^2 - g(p_0^h)^2(c_0^h)^2 - b(c_0^h)^4)}{p_1^2(3a_1^h + a_0^h)}. \quad (15)$$

In fig. 4 we show the effect of the deformation parameter b on the reduced free energy density $\hat{\mathcal{F}}^b$ of the symmetry broken phase in the QFT_3^b model, compare to the corresponding free energy density in the QFT_3 model, denoted by $\hat{\mathcal{F}}^0$ (this is the solid magenta curve in the left panel of fig. 1). The dashed curve corresponds to $b = 1$ and the dotted curve corresponds to $b = -1$. They originate from the same green dot, representing the critical temperature T_{crit} , as in (11). Following the symmetry broken phases in the QFT_3^b model to infinitely high temperature, we identify conformal phases, CFT_3^b , with the spontaneously broken $\mathbb{Z}_2 \times \mathbb{Z}_2$ global symmetry — these are the two black dots in fig. 4. Since we want to reduced the free energy density as much as possible, we now study CFT_3^b models for $b < 0$ ¹⁰.

⁹Of course, all the UV and IR parameters $\{p_2, \chi_4, a_0^h, a_1^h, p_0^h, c_0^h\}$ will develop an implicit b dependence.

¹⁰Notice that the gravitational scalar potential in (14) is unbounded for $b < 0$. This does not immediately signal any pathologies — many scalar potentials in top-down supersymmetric holographic models are unbounded. See [4] for further discussion.

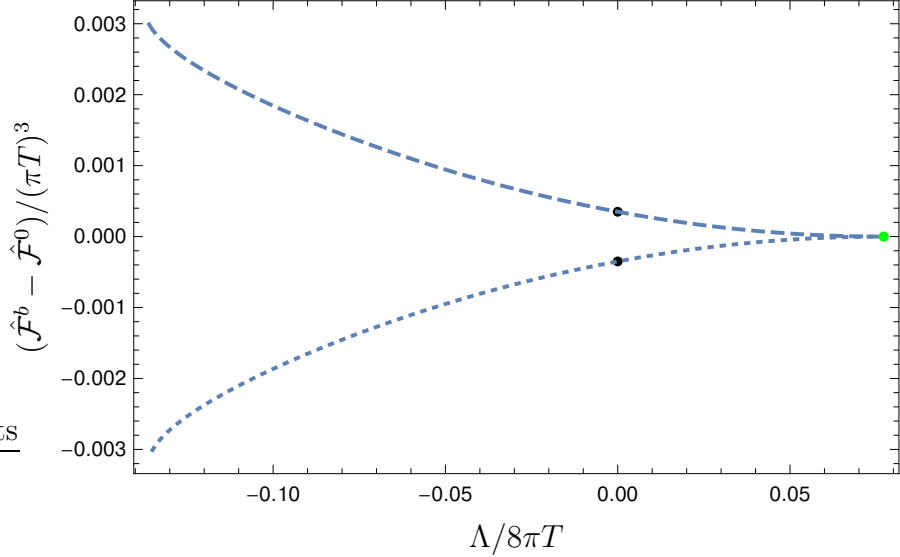


Figure 4: The reduced free energy densities $\hat{\mathcal{F}}^b$ of the \mathbb{Z}_2 symmetry broken thermal phases of the QFT_3^b model, see (14), compare to the free energy density $\hat{\mathcal{F}}^0$ of the corresponding phases of the QFT_3 model, see (1). The dashed curve corresponds to $b = 1$ and the dotted curve corresponds to $b = -1$ deformation parameter. The green dot indicates the b -independent critical temperature T_{crit} , see (11). The black dots represent new examples of CFT_3^b with spontaneously broken $\mathbb{Z}_2 \times \mathbb{Z}_2$ global symmetry.

In fig. 5 we follow (the solid black curve) the free energy density in the CFT_3^b model from $b = 0$ (represented by the black dot — the same black dot as in fig. 1) for $b < 0$. The horizontal red line is the value of the free energy density for the AdS_4 -Schwarzschild black brane, see (10). We find that the CFT_3^b model allows for a symmetry broken phase only for

$$b \geq b_{crit} = -122.272. \quad (16)$$

The critical value of the deformation parameter is denoted by a vertical dashed blue line.

The origin of b_{crit} is easy to understand as we follow the symmetry breaking order parameters $\langle \hat{\mathcal{O}}_r \rangle$ and $\langle \hat{\mathcal{O}}_i \rangle$ in the CFT_3^b model, see fig. 6. We find that while $\langle \hat{\mathcal{O}}_i \rangle$ remains finite in the limit $b \rightarrow b_{crit}$,

$$\langle \hat{\mathcal{O}}_r \rangle \propto (b - b_{crit})^{1/2}. \quad (17)$$

Thus, precisely at $b = b_{crit}$ the black brane dual to the CFT_3^b symmetry broken phase

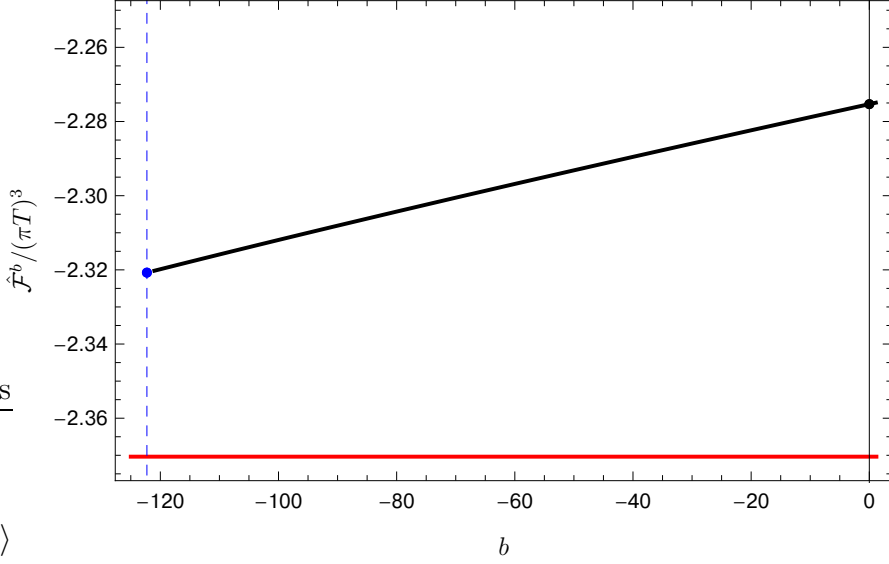


Figure 5: The reduced free energy density $\hat{\mathcal{F}}^b$ in the CFT_3^b model as a function of the deformation parameter b (the solid black line). The black dot represents the same symmetry broken conformal phase as the black dot in fig. 1. The CFT_3^b symmetry broken phase exists only for $b \geq b_{crit}$, see (16), denoted by a vertical dashed blue line — it terminates with a blue dot CFT_3^ψ , see (18). The horizontal red line represents the reduced free energy density of the AdS_4 -Schwarzschild black brane.

”losses” the ϕ -hair, while maintaining the non-vanishing ψ -hair. We call this ”terminal” conformal model CFT_3^ψ ,

$$\begin{aligned} \text{CFT}_3^\psi \Big|_{b=b_{crit}} &\equiv \lim_{b \rightarrow b_{crit}} \text{CFT}_3^b, \\ \text{CFT}_3^\psi \Big|_{b=b_{crit}} : \quad \frac{\hat{\mathcal{F}}^\psi}{(\pi T)^3} \Big|_{b=b_{crit}} &= -2.32074, \quad \langle \hat{\mathcal{O}}_i \rangle \Big|_{b=b_{crit}} = \pm 0.21057, \end{aligned} \quad (18)$$

where again the \pm signs indicate the 2-fold degeneracy due to the spontaneously broken \mathbb{Z}_2 global symmetry.

Once again,

$$\frac{\hat{\mathcal{F}}^\psi}{(\pi T)^3} \Big|_{b=b_{crit}} > \frac{\hat{\mathcal{F}}}{(\pi T)^3} \Big|_{AdS_4-\text{Schwarzschild}}. \quad (19)$$

Can we do better with relaxing $b = b_{crit}$ constraint directly in the CFT_3^ψ model? This leads us to **Step3**.

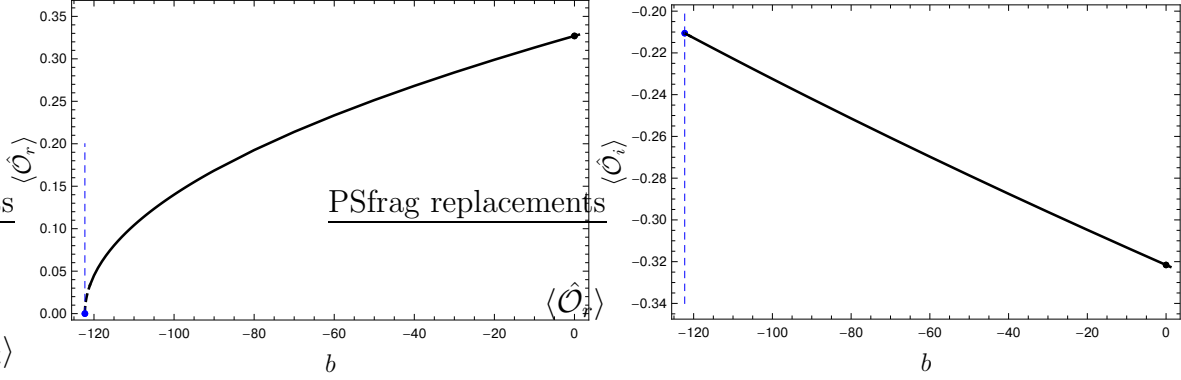


Figure 6: The symmetry breaking order parameters $\langle \hat{\mathcal{O}}_r \rangle$ and $\langle \hat{\mathcal{O}}_i \rangle$ in the CFT_3^b model as a function of b . The $\langle \hat{\mathcal{O}}_r \rangle$ order parameter vanishes as $b \rightarrow b_{\text{crit}}$, denoted by the vertical dashed blue lines. However, the $\langle \hat{\mathcal{O}}_i \rangle$ order parameter remains finite at $b = b_{\text{crit}}$ (the blue dot).

- **Step3.** Consider a gravitational dual to CFT_3^ψ model,

$$S_{\text{CFT}_3^\psi} = \frac{1}{2\kappa^2} \int dx^4 \sqrt{-\gamma} \left[R + 6 - \frac{1}{2} (\nabla\chi)^2 - 2\chi^2 - b\chi^4 \right], \quad (20)$$

Clearly, the $S_{\text{CFT}_3^\psi}$ model is a consistent truncation of the $S_{\text{QFT}_3^b}$ model with $\phi \equiv 0$. The CFT_3^ψ model has only \mathbb{Z}_2 global symmetry. The symmetry broken blue dot phase in fig. 5 must also be a solution of the effective action (20), except that now we are not restricted to keep $b = b_{\text{crit}}$.

The thermal phase with the spontaneously broken \mathbb{Z}_2 symmetry exists in the CFT_3^ψ model for $b \leq -\frac{3}{2}$, see fig. 8.

As $b \rightarrow -\frac{3}{2}$, the order parameter for the symmetry breaking diverges as, see fig. 9,

$$|\langle \hat{\mathcal{O}}_i \rangle| \propto \frac{1}{-3/2 - b}, \quad \text{as} \quad b \rightarrow -\frac{3}{2}. \quad (21)$$

Notice that

$$\frac{\hat{\mathcal{F}}^\psi}{(\pi T)^3} > \frac{\hat{\mathcal{F}}}{(\pi T)^3} \Big|_{AdS_4-\text{Schwarzschild}}, \quad (22)$$

for all value of b , see fig 10. We find that as $b \rightarrow -\infty$,

$$\frac{\hat{\mathcal{F}}^\psi}{(\pi T)^3} = \frac{\hat{\mathcal{F}}}{(\pi T)^3} \Big|_{AdS_4-\text{Schwarzschild}} + \mathcal{C} \exp b, \quad |\langle \hat{\mathcal{O}}_i \rangle| \propto \frac{1}{\sqrt{-b}}, \quad (23)$$

where $\mathcal{C} \approx 1.81$.

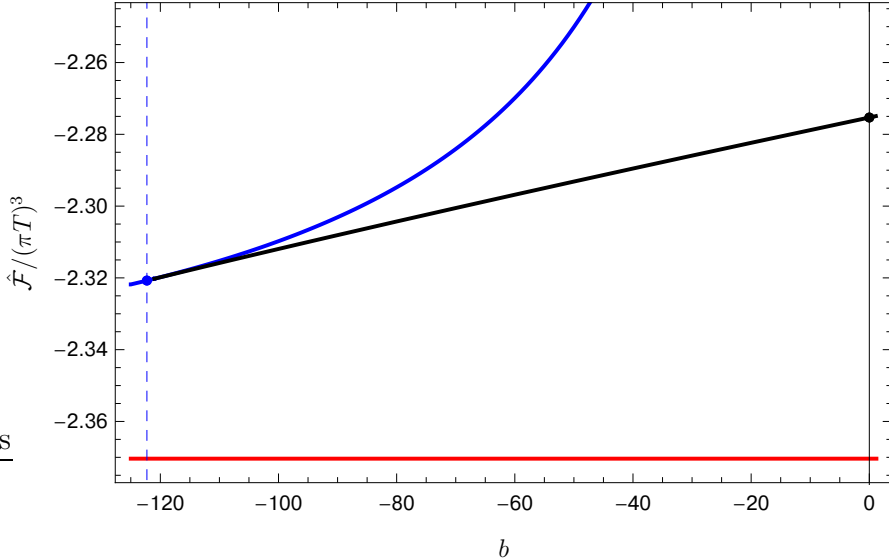


Figure 7: Same as in fig. 5, with the addition of the symmetry breaking phase in the CFT_3^ψ model, see (20) — the solid blue curve.

Acknowledgments

Research at Perimeter Institute is supported by the Government of Canada through Industry Canada and by the Province of Ontario through the Ministry of Research & Innovation. This work was further supported by NSERC through the Discovery Grants program.

References

- [1] N. Chai, S. Chaudhuri, C. Choi, Z. Komargodski, E. Rabinovici and M. Smolkin, *Thermal Order in Conformal Theories*, 2005.03676.
- [2] A. Buchel and C. Pagnutti, *Exotic Hairy Black Holes*, *Nucl. Phys. B* **824** (2010) 85–94, [0904.1716].
- [3] P. Bosch, A. Buchel and L. Lehner, *Unstable horizons and singularity development in holography*, *JHEP* **07** (2017) 135, [1704.05454].
- [4] A. Buchel, *Singularity development and supersymmetry in holography*, *JHEP* **08** (2017) 134, [1705.08560].

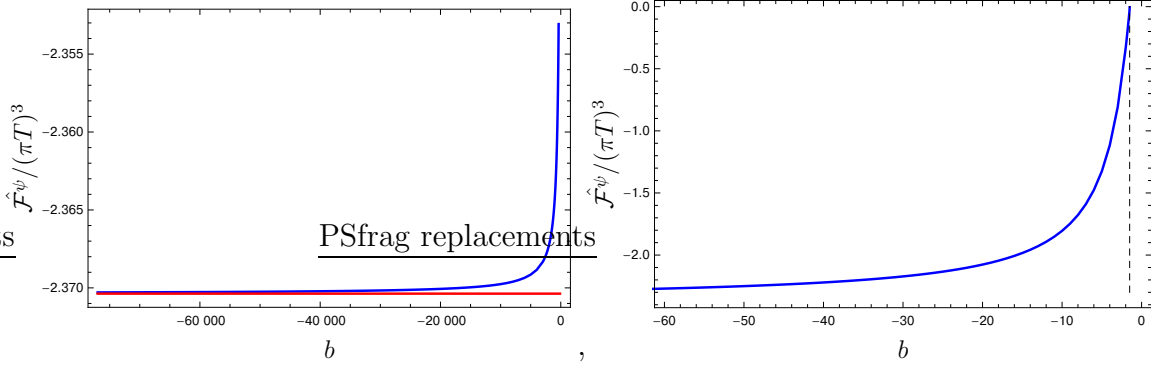


Figure 8: The reduced free energy density $\hat{\mathcal{F}}^\psi$ of the \mathbb{Z}_2 symmetry broken phase as a function of b . This phase exists only for $b < -\frac{3}{2}$, represented by a vertical dashed black line in the right panel. The horizontal red line represents the reduced free energy density of the AdS_4 -Schwarzschild black brane.

- [5] A. Buchel, *Klebanov-Strassler black hole*, *JHEP* **01** (2019) 207, [1809.08484].
- [6] I. R. Klebanov and M. J. Strassler, *Supergravity and a confining gauge theory: Duality cascades and chi SB resolution of naked singularities*, *JHEP* **08** (2000) 052, [hep-th/0007191].
- [7] A. Buchel, *A Holographic perspective on Gubser-Mitra conjecture*, *Nucl. Phys.* **B731** (2005) 109–124, [hep-th/0507275].

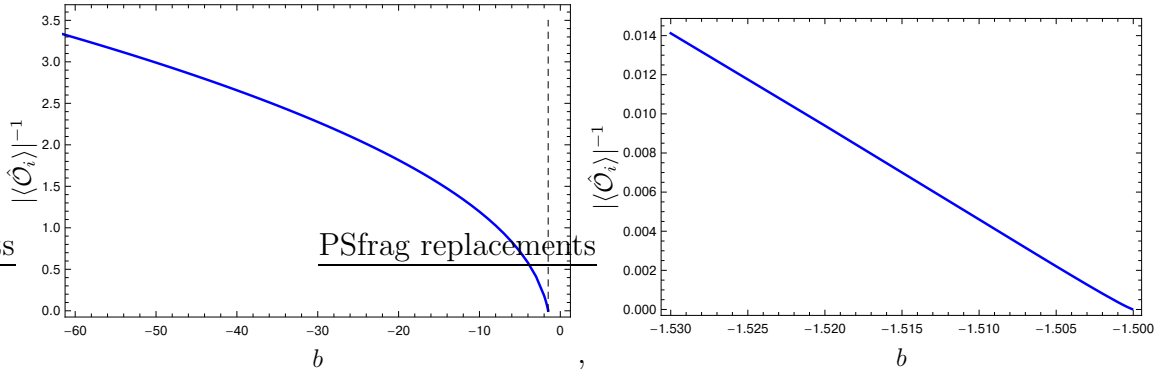


Figure 9: The inverse of the order parameter $|\langle \hat{O}_i \rangle|$ for the symmetry breaking in the CFT_3^ψ model as $b \rightarrow -\frac{3}{2}^-$.

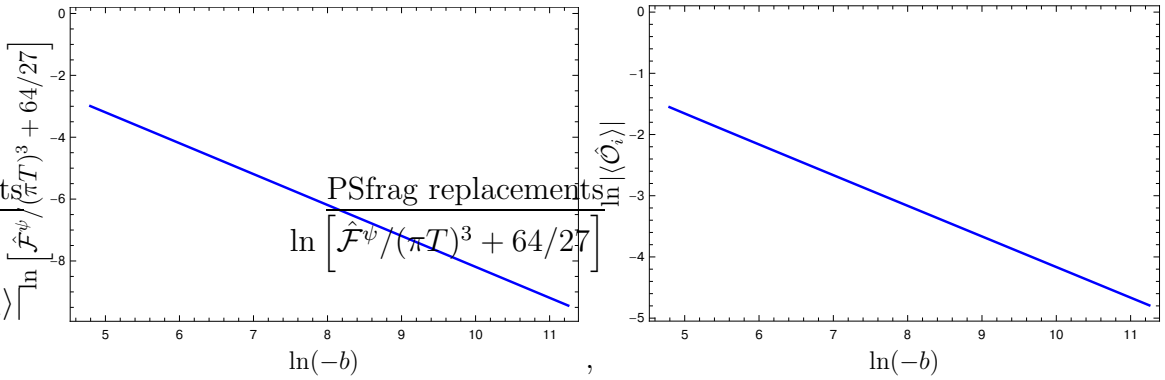


Figure 10: The reduced free energy density of the symmetry broken phase in the CFT_3^ψ model always exceeds that of the symmetric phase. It approaches the latter as $\propto \exp b$ in the limit $(-b) \rightarrow \infty$, see the left panel. In the right panel we show the $\propto (-b)^{-1/2}$ scaling of the symmetry breaking order parameter in the CFT_3^ψ model in the limit $(-b) \rightarrow \infty$.